ChemComm

COMMUNICATION

View Article Online
View Journal | View Issue

Open Access Article. Published on 27 January 2016. Downloaded on 8/16/2024 10:47:37 AM.
This article is licensed under a Creative Commons Attribution-NonCommercial 3.0 Unported Licence.

Cite this: *Chem. Commun.*, 2016, 52, 3500

Received 17th December 2015,
Accepted 27th January 2016

DOI: 10.1039/c5cc10363k

www.rsc.org/chemcomm

On the nature of the stabilisation of the E···π pnicogen bond in the $SbCl_3$···toluene complex†

Rabindranath Lo,[a] Petr Švec,[b] Zdeňka Růžičková,[b] Aleš Růžička[b] and Pavel Hobza*[ac]

The off-symmetrical structure of the toluene···$SbCl_3$ complex is a consequence of the off-centre location of σ-holes at the Sb atom. DFT-SAPT calculations have been used to determine the total interaction energies and their components. The characteristic features of the pnicogen bonding are due to the concert action of electrostatic and dispersion interactions.

Although the existence of σ-hole bonding is definitely not new, its appearance in crystals is still surprising, because it is counterintuitive. This is also true about pnicogen (Pn) bonding, *i.e.* the bonding involving Group VA elements (N, P, As, Sb and Bi). The first experimental evidence on the P···P pnicogen bond already appeared at the end of the 1970s,[1] the first theoretical evidence followed in the mid-1990s,[2] and this bonding was fully recognised at the beginning of the 2010s.[3] What was surprising was not the existence of the P···P pnicogen bond but the fact that it can be as strong as the far better known H-bond. The Pn···Y pnicogen bond (like all the other σ-hole bonds) is a bond between a positively charged σ-hole in pnicogens and a negatively charged electron donor Y (*e.g.* O or N) or π electrons in unsaturated hydrocarbons and aromatic molecules.[4] The very existence of all σ-hole bonds arises from the presence of a σ-hole at atoms of Groups IV, V, VI, VII and VIII which are covalently bound to an electronegative atom, mostly carbon. The σ-hole originates in an unequal occupation of valence orbitals and is thus of quantum origin. The mere fact that the electron density of an atom is not spherically symmetric is of key importance and, among other things, it means that one of the pillars of molecular mechanics, spherically symmetric electron density, is not applicable for a large portion of the periodic table.

A σ-hole is characterised by its magnitude ($V_{s,max}$) and size,[5] the former of which is defined as the value of the most positive electrostatic potential (ESP) of an electron density surface while the latter as the spatial extent of the positive region. The tunability of a σ-hole is one of its important properties and both the magnitude and the size increase with atomic size and also through the substitution of suitable atoms or groups. The strength of a σ-hole bond is proportional to its magnitude. For monovalent atoms, like halogens, there is only one σ-hole localised opposite a C–X covalent bond. Consequently, the C–X···Y angle in halogen-bonded complexes is close to 180° and the halogen bond is significantly more directional than the better known H-bond. Generally, the directionality of the halogen bond is determined by the gradient of the ESP[6] and it increases when going from Cl to I. When, however, an atom having a σ-hole is polyvalent, then more than one σ-hole is localised, again at the side opposite to the corresponding covalent bond. Such an arrangement is not consistent with the linearity of the bond and it must have consequences on the structure of the crystal. We have recently demonstrated[7] it for the crystal of the Ph-*closo*-1-$SB_{11}H_{10}$, having pentavalent sulphur, where the B–S···π chalcogen bond has been found to be bent in full agreement with the predicted off-centre location of the sulphur σ-holes. The respective chalcogen bond has been found to be surprisingly strong, more than 8 kcal mol^{-1}, and the most dominant contribution to the overall stabilisation energy originates in dispersion energy.

Pnicogens are mostly trivalent, as a result of which three σ-holes will be localised at the belt of pnicogens. This is apparent in Fig. 1, showing the ESP of the $SbCl_3$ molecule. Evidently, deep blue σ-holes are localised at the belt of the Sb atom. These σ-holes are of surprisingly high magnitude, 48.0 kcal mol^{-1}, which is considerably more than the magnitude of the σ-hole in most halogen- and chalcogen-containing systems. The top of the Sb

[a] *Institute of Organic Chemistry and Biochemistry, Academy of Sciences of the Czech Republic, v.v.i., Flemingovo nám. 2, 166 10 Prague 6, Czech Republic. E-mail: hobza@uochb.cas.cz*
[b] *Department of General and Inorganic Chemistry, Faculty of Chemical Technology, University of Pardubice, Studentská 573, CZ-532 10, Pardubice, Czech Republic*
[c] *Regional Centre of Advanced Technologies and Materials, Department of Physical Chemistry, Palacký University, 771 46 Olomouc, Czech Republic*

† Electronic supplementary information (ESI) available: Computational details and the coordinates of the optimized geometries, electron differential map and selected parameters of crystallographic measurements. CCDC 1432791. For ESI and crystallographic data in CIF or other electronic format see DOI: 10.1039/c5cc10363k

This journal is © The Royal Society of Chemistry 2016

Open Access Article. Published on 27 January 2016. Downloaded on 8/16/2024 10:47:37 AM.
This article is licensed under a Creative Commons Attribution-NonCommercial 3.0 Unported Licence.

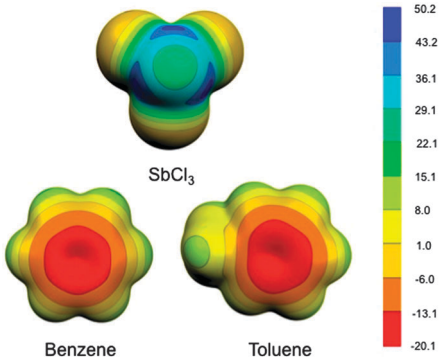

Fig. 1 Computed electrostatic potentials on 0.001 a.u. molecular surfaces of $SbCl_3$, benzene and toluene. The colour of the ESP ranges in kcal mol^{-1}. The figure was prepared with MOLEKEL.

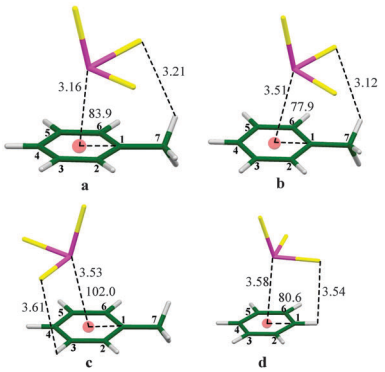

Fig. 2 The crystal (a) and optimised (b) (DFT-D3/BLYP/def2-TZVPP level) geometries of the global and local (c) minima of toluene···$SbCl_3$ complexes. (d) The optimised structure of the benzene···$SbCl_3$ complex. The distances are given in Å and the angles in degrees. Atom colour coding: [C: green; H: white; Sb: magenta; Cl: yellow].

atom is still positive but considerably less (24.9 kcal mol^{-1}). Substitution of chlorines by fluorines, bromines or iodines leads to increased/decreased magnitudes of the respective σ-hole: 58.7, 44.5 and 37.9 kcal mol^{-1}, respectively. Furthermore, substitution of Sb in $SbCl_3$ by As and Bi results in σ-hole magnitudes of 38.0 and 59.5 kcal mol^{-1}, respectively. On the basis of a highly positive magnitude of the σ-hole, one can expect high stabilisation energies of the respective complexes with the pnicogen bond. The off-centre localisation of σ-holes in $SbCl_3$ determines the structure of complexes with $SbCl_3$. Due to the absence of gas-phase structures of pnicogen-bonded complexes, the respective crystal structures are an important source of information on this novel type of noncovalent interaction.

The aim of the present communication is twofold: first to investigate the structure and geometry of the toluene···$SbCl_3$ complex and, second, to study the nature of the σ-hole (Sb) pnicogen bond. This study thus complements our previous studies on the nature of stabilisation in halogen and chalcogen bonding.

We have tried to prepare a plethora of complexes of aromatic hydrocarbons with various group 15 element trihalides in different molar ratios, thus following the initial chemistry of Menshutkin,[8] which was further developed by Schmidbaur, Müller and others.[9] Unfortunately, we were able to isolate and crystallographically characterise only eight complexes (seven of which were almost identical, in terms of unit cell parameters and the structure, to the already published ones). The only new compound under investigation was a 1 : 1 $SbCl_3$–toluene adduct, which does not seem to be thermally stable, because its melting point (∼−23 °C) is about 130 °C lower than for other known complexes. It seems that this instability was also the reason for previous failures in its synthesis, isolation and characterisation. The fact that a usual synthetic setup uses toluene as a solvent for the preparation of the rest of the respective complexes also implies the labile character of the atom–aromatic ring connection. The adduct is composed of the $SbCl_3$ moiety asymmetrically bound to the toluene molecule (*cf.* Fig. 2a and Fig. S1, ESI†). Toluene is most likely to interact with the antimony atom in a η^3-fashion; its projection is moved from the centre of gravity of the aromatic six-membered ring towards the carbon atom connected to the methyl group. The distance between an η^3-centroid (C1, C2, C3) and Sb1, 3.193(4) Å, is similar to the distances found between the Sb atoms and η^3-centroids of aromatic rings in the reported complexes with either inverse sandwich or piano stool structures.[9] Two of covalent Sb–Cl bonds lie in the plane parallel to the plane defined by the toluene molecule, while the third bond is perpendicular to it in the geometry of a distorted seesaw. The coordination polyhedra of antimony atoms are further completed by additional three chlorine atoms tri-capping each Sb atom in the plane parallel to the plane of the toluene molecule (Fig. S1–S6, ESI†), where the contacts between the antimony and those three atoms are extremely elongated (3.462(2)–3.724(3) Å, Fig. S6, ESI†) in comparison with the covalently bound ones (2.357(3) for Cl in the *trans* position to the toluene centroid, 2.371(3) and 2.375(3) Å for Cl atoms in the parallel plane, Fig. S6, ESI†). Moreover, the Cl–Cl contact of 3.378(4) Å in the counterintuitive geometry is observed in the supramolecular architecture of the crystal (Fig. S6, ESI†). This short contact is most probably constrained by the contacts of both Cl atoms to the same antimony in a triangular fashion (Fig. S2–S6, ESI†).

The crystal structure of toluene···$SbCl_3$ differs from that of benzene···$SbCl_3$, which is a consequence of a different electrostatic potential. Fig. 1 shows the ESP of toluene and benzene. The introduction of an electron-donating methyl group has increased the electron density above the aromatic ring (from −18.4 to −20.0 kcal mol^{-1}) and shifted the maximum away from the Me group (by 0.4 Å). The higher electron density in the case of the toluene complex (with respect to the benzene complex) will result in a higher stabilisation energy of the toluene complex. The X-ray structure of the toluene···$SbCl_3$ complex is shown in Fig. 2a, and the belt structure is mainly caused by the interaction of the antimony off-centre σ-hole with aromatic π-electrons. The fact that it is this interaction (and not other secondary crystal interactions) that determines the structure of the toluene···$SbCl_3$ complex is evident from the structure resulting from the full optimisation of the mere dimer (Fig. 2b). The structural features of this structure are the same,

Open Access Article. Published on 27 January 2016. Downloaded on 8/16/2024 10:47:37 AM.
This article is licensed under a Creative Commons Attribution-NonCommercial 3.0 Unported Licence.

with only the intermolecular distance being larger. Both structures exhibit contacts between the chlorine atoms of $SbCl_3$ and the hydrogen atoms of the methyl group of toluene. The electrostatic attraction between these atoms is responsible for the geometry change, specifically by diminishing the C1–(toluene/benzene centre of mass)–Sb valence angle when going from the benzene to the toluene complex (from 80.6 to 77.9 degrees). The reduction of the angle found for the optimised structures qualitatively agrees with that detected in crystal structures (2.7° *vs.* 0.4°, respectively). When investigating the crystal structure (**2a**), we further detected an elongation of the aromatic C1–C2 bond, which is the longest in the phenyl ring. A similar elongation was also found in the optimised structure (**2b**). To explain this, we performed the Natural Bond Order (NBO) analysis, which pointed out the charge transfer $\sigma_{C1-C2} \rightarrow \sigma^*_{Sb-Cl}$ and to a lesser extent $n_{Cl} \rightarrow \sigma^*_{C1-C6}$ also. The weakening of the C1–C2 and C1–C6 bonds (resulting from a decrease of electron density in the C1–C2 bonding and an increase of electron density in C1–C6 antibonding orbitals, respectively) leads to their elongation in full agreement with the experiment.

The structure shown in Fig. 2b corresponds to the global minimum while that in Fig. 2c to the less stable local minimum. The dispersion energy is clearly dominant in the stabilisation of both structures; it forms 6.9 and 5.3 kcal mol^{-1} from the total stabilisation of 8.0 and 6.8 kcal mol^{-1} for the global and local minimum structures, respectively. Furthermore, the dispersion energy is higher (more negative) for the global minimum, which is evidently caused by the fact that here the contact between the heavy atoms of the pnicogen and the methyl group of toluene is larger than that for the other structure. Finally, the repulsion force between the lone pair on the Sb atom and the π-electrons of the aromatic ring should be taken into consideration.[10]

We are certainly aware of the fact that the structure of the dimer is affected also by factors other than electrostatic attraction between the σ-holes with aromatic π-electrons. To elucidate the role of other contributions we used the noncovalent interaction method introduced by Yang *et al.*[11] The noncovalent interaction (NCI) index is a beneficial approach to distinguish and visualize various types of noncovalent interactions in real space. It is based on the relationship between electron density (ρ) and its derivatives with the reduced density gradient (RDG). RDG is a fundamental dimensionless quantity generated from the density and its first derivatives.[11] Fig. 3 shows RDG *vs.* sign(λ_2)ρ for the toluene···$SbCl_3$ complex. ρ determines the strength of interaction and sign(λ_2), the sign of λ_2 is capable of differentiating the types of interaction. Hence, it is deliberated that the high value of ρ and the negative sign of sign(λ_2) indicate the attractive interaction, while a high value of ρ and a positive sign of sign(λ_2) suggest that the interaction is nonbonding.[11] The scatter plot in Fig. 3 shows the low density, low-gradient spikes lying at negative regions, which indicates the stabilization interactions in the pnicogen complex. The most negative spike describes the pnicogen bond between σ-hole and aromatic π-electrons while two low density spikes very close to zero correspond to additional noncovalent interactions between negatively charged chlorines and positively charged methyl hydrogens (*cf.* reduced gradient isosurface in Fig. 3b).

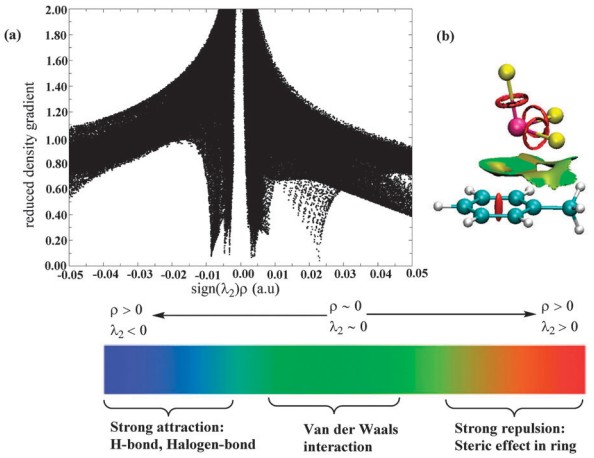

Fig. 3 (a) Plot of the reduced density gradient *versus* the electron density multiplied by the sign of the second Hessian eigenvalue, (b) bonding isosurface for the toluene···$SbCl_3$ complex.

The decomposition of the total interaction energy can help to elucidate the nature of the stabilisation of the particular complex; the present splitting of the total stabilisation energy into dispersion and DFT parts is not reliable enough. The most reliable decomposition is obtained by using the DFT-SAPT technique.[12] The total interaction energy is constructed as the sum of polarisation/electrostatic, exchange-repulsion, induction and dispersion energies, where induction and dispersion energies are constructed as the sum of parent and respective exchange parts. Furthermore, induction energy also includes the δHF term. Table 1 shows the total DFT-SAPT energy and its components for the complexes investigated. Notice that the dispersion energies of all the complexes were scaled by 1.14, which is the ratio between the dispersion energies of the benzene···$SbCl_3$ complex determined using aug-cc-pVDZ and aug-cc-pVTZ basis sets. All the other terms, determined using a smaller basis set, are not sensitive to the basis-set size. The DFT-SAPT total interaction energy for both structures of the toluene···$SbCl_3$ complex is higher (more negative) than the DFT-D3 value, which is mainly due to the underestimation of D3 dispersion energy. The DFT-SAPT dispersion energies calculated using the aug-cc-pVTZ basis set are clearly more reliable. For both structures of the toluene···$SbCl_3$ complex, the dispersion energy is the highest, followed by polarisation/electrostatic energy; the induction energy is much low. Difference between dispersion and polarization/electrostatic energies is, however, not dramatic. The stabilisation energy of the complex

Table 1 DFT-SAPT interaction energies and their components (in kcal mol^{-1}) for the global (b) and local (c) minima of the toluene···$SbCl_3$ complex and the global minimum of the benzene(ben)···$SbCl_3$ and hexamethylbenzene (hexametben)···$SbCl_3$ complexes

Structure		ΔE	E_1^{Pol}	E_1^{exch}	$E^{disp\,a}$	$E^{ind\,a}$
Tol···$SbCl_3$	**2b**	−9.6	−7.5	9.6	−9.0	−2.6
	2c	−8.5	−6.7	7.8	−7.2	−2.4
Ben···$SbCl_3$		−7.7	−6.1	7.1	−6.7	−2.0
Hexametben···$SbCl_3$		−15.5	−13.0	17.5	−14.3	−5.7

[a] $E^{disp} = E_2^{disp} + E_2^{exch\text{-}disp}$; $E^{ind} = E_2^{ind} + E_2^{exch\text{-}ind} + \delta HF$.

 This journal is © The Royal Society of Chemistry 2016

Open Access Article. Published on 27 January 2016. Downloaded on 8/16/2024 10:47:37 AM.
This article is licensed under a Creative Commons Attribution-NonCommercial 3.0 Unported Licence.

is substantial and the question is what role is played by the presence of the electron-donated methyl group. Table 1 shows the DFT-SAPT total interaction energy and its components for the benzene···$SbCl_3$ complex determined at the same level. The total interaction energy and dispersion energy of the complex are 20 and 25% lower than those of the toluene complex; also for the benzene complex, the dispersion energy is the dominant energy term. Evidently, the role of methyl substitution is not fundamental and already the stabilisation energy of the benzene complex is substantial. A dramatic increase of all energies was obtained upon permethylation of the benzene system. It is observed from Table 1 that the total stabilisation energy as well as the dispersion energy with respect to the toluene complex dramatically increased now (by 61 and 59%, respectively). Also for this complex, the dispersion energy has a dominant stabilisation contribution and its relative weight (92%) is similar to that of toluene and benzene (see Fig. 2d) complexes (94 and 87%, respectively). In the case of the toluene complex, polarisation/electrostatic energy contributes by 78% to the total stabilisation, and this ratio does not change much when passing to benzene and hexamethylbenzene complexes (79 and 84%, respectively). All of these numbers show that the nature of stabilisation in toluene, benzene and hexamethybenzene complexes is similar; in all the cases, the leading dispersion energy is followed by polarisation/electrostatic and induction energies. A dominant role of dispersion energy is slightly surprising since due to a very high magnitude of the respective σ-holes we expected a dominant role of polarization/electrostatic energy. The magnitude of dispersion energy is conditioned by the close contact of the heavy and polarizable Sb atom with the atoms of toluene, benzene or hexamethylbenzene. It should be mentioned here that the IUPAC definition[13] of halogen bonding emphasises the role of electrostatic energy, whereas the SAPT decomposition of halogen-bonded complexes[14] as well as of the present pnicogen complexes favours comparable role of both polarization/electrostatic and dispersion energies.

It can be concluded that the off-symmetrical structure of the toluene···$SbCl_3$ complex is caused by the off-centre location of the σ-holes at the Sb atom. The structure of the complex (as well as of the related complexes investigated) is thus mainly determined by the electrostatic attraction between the positive σ-hole of the Sb atom and the negative π-electrons of the aromatic ring while their high stabilisation energies are due to both polarization/electrostatic and the dispersion energies. The characteristic features of pnicogen bonding are thus a result of the concert action of attractive dispersion and electrostatic interactions as well as of low exchange-repulsion interaction originating in polar flattening[15] of pnicogen atoms in the pnicogen bond. A similar situation was found in previously investigated halogen and chalcogen bonding.

This work was part of the Research Project RVO: 61388963 of the Institute of Organic Chemistry and Biochemistry, Academy of Sciences of the Czech Republic. This work was also supported by the Czech Science Foundation [P208/12/G016, P207/12/0223]. The authors gratefully acknowledge the support by the project LO1305 of the Ministry of Education, Youth and Sports of the Czech Republic.

Notes and references

1 W. E. Hill and L. M. Silva-Trivino, *Inorg. Chem.*, 1979, **18**, 361.
2 K. W. Klinkhammer and P. Pyykkö, *Inorg. Chem.*, 1995, **34**, 4134.
3 S. Zahn, R. Frank, E. Hey-Hawkins and B. Kirchner, *Chem. – Eur. J.*, 2011, **17**, 6034.
4 (*a*) X.-L. An, R. Li, Q.-Z. Li, X.-F. Liu, W.-Z. Li and J.-B. Cheng, *J. Mol. Model.*, 2012, **18**, 4325; (*b*) H. Xu, W. Wang and J. Zou, *Acta Chim. Sin.*, 2013, **71**, 1175; (*c*) A. Bauzá, D. Quiñonero, P. M. Deyà and A. Frontera, *CrystEngComm*, 2013, **15**, 3137; (*d*) A. Bauzá, D. Quiñonero, P. M. Deyà and A. Frontera, *Phys. Chem. Chem. Phys.*, 2012, **14**, 14061.
5 M. Kolář, J. Hostaš and P. Hobza, *Phys. Chem. Chem. Phys.*, 2014, **16**, 9987.
6 M. Kolář, J. Hostaš and P. Hobza, *Phys. Chem. Chem. Phys.*, 2015, **17**, 23279.
7 J. Fanfrlík, A. Přáda, Z. Padělková, A. Pecina, J. Macháček, M. Lepšík, J. Holub, A. Růžička, D. Hnyk and P. Hobza, *Angew. Chem., Int. Ed.*, 2014, **53**, 10139.
8 (*a*) B. N. Menshutkin, *J. Russ. Phys. – Chem. Soc.*, 1911, **43**, 1294; (*b*) B. N. Menshutkin, *J. Russ. Phys. – Chem. Soc.*, 1911, **43**, 1805; (*c*) B. N. Menshutkin, *J. Russ. Phys. – Chem. Soc.*, 1912, **44**, 1079.
9 (*a*) For a review, see: H. Schmidbaur and A. Schier, *Organometallics*, 2008, **27**, 2361; (*b*) for selected references, see: A. Schier, J. M. Wallis, G. Müller and H. Schmidbaur, *Angew. Chem., Int. Ed. Engl.*, 1986, **25**, 757; (*c*) H. Schmidbaur, R. Nowak, O. Steigelmann and G. Müller, *Chem. Ber.*, 1990, **123**, 1221; (*d*) A. Lipka and D. Mootz, *Z. Anorg. Allg. Chem.*, 1978, **440**, 217; (*e*) N. Burford, J. A. C. Clyburne, J. A. Wiles, T. S. Cameron and K. N. Robertson, *Organometallics*, 1996, **15**, 361; (*f*) D. Mootz and V. Handler, *Z. Anorg. Allg. Chem.*, 1986, **533**, 23; (*g*) T. Probst, O. Steigelmann, J. Riede and H. Schmidbaur, *Chem. Ber.*, 1991, **124**, 1089.
10 A. J. Stone, *J. Am. Chem. Soc.*, 2013, **135**, 7005.
11 (*a*) J. Contreras-García, E. R. Johnson, S. Keinan, R. Chaudret, J.-P. Piquemal, D. N. Beratan and W. Yang, *J. Chem. Theory Comput.*, 2011, **7**, 625; (*b*) E. R. Johnson, S. Keinan, P. Mori-Sanchez, J. Contreras-Garcia, A. J. Cohen and W. Yang, *J. Am. Chem. Soc.*, 2010, **132**, 6498.
12 (*a*) B. Jeziorski, R. Moszynski and K. Szalewicz, *Chem. Rev.*, 1994, **94**, 1887; (*b*) G. Jansen and A. Hesselmann, *J. Phys. Chem. A*, 2001, **105**, 11156; (*c*) A. Hesselmann, G. Jansen and M. Schutz, *J. Chem. Phys.*, 2005, **122**(1), 014103; (*d*) A. Hesselmann and G. Jansen, *Chem. Phys. Lett.*, 2002, **357**, 464; (*e*) A. Hesselmann, G. Jansen and M. Schutz, *J. Am. Chem. Soc.*, 2006, **128**, 11730; (*f*) A. Hesselmann and G. Jansen, *Chem. Phys. Lett.*, 2003, **367**, 778; (*g*) A. Hesselmann and G. Jansen, *Chem. Phys. Lett.*, 2002, **362**, 319; (*h*) H. L. Williams and C. F. Chabalowski, *J. Phys. Chem. A*, 2001, **105**, 646; (*i*) A. J. Misquitta and K. Szalewicz, *Chem. Phys. Lett.*, 2002, **357**, 301; (*j*) R. Podeszwa, R. Bukowski and K. Szalewicz, *J. Phys. Chem. A*, 2006, **110**, 10345; (*k*) S. Rybak, K. Szalewicz, B. Jeziorski and G. Corongiu, *Chem. Phys. Lett.*, 1992, **199**, 567.
13 G. R. Desiraju, P. S. Ho, L. Kloo, A. C. Legon, R. Marquardt, P. Metrangolo, P. Politzer, G. Resnati and K. Rissanen, *Pure Appl. Chem.*, 2013, **85**, 1711.
14 M. H. Kolář, P. Deepa, H. Ajani, A. Pecina and P. Hobza, *Top. Curr. Chem.*, 2015, **359**, 1.
15 R. Sedlak, M. H. Kolář and P. Hobza, *J. Chem. Theory Comput.*, 2015, **11**, 4727.